

# A NEW DOUBLE DECONVOLUTION METHOD SUITABLE FOR NON-STATIONARY SEISMOGRAMS IN THE TIME-FREQUENCY DOMAIN

RONG-RONG WANG<sup>1</sup>, YONG-SHOU DAI<sup>1</sup>, CHUANG LI<sup>2</sup>, PENG ZHANG<sup>1</sup>  
and YONG-CHENG TAN<sup>1</sup>

<sup>1</sup> College of Information and Control Engineering, China university of Petroleum (East China), Qingdao 266580, P.R. China. 913290023@qq.com

<sup>2</sup> Department of Geophysics, China University of Petroleum (East China), Qingdao 266580, P.R. China.

(Received February 1, 2015; revised version accepted June 2, 2015)

## ABSTRACT

Wang, R.-R., Dai, Y.-S., Li, C., Zhang, P. and Tan, Y.-C., 2015. A new double deconvolution method suitable for non-stationary seismograms in the time-frequency domain. *Journal of Seismic Exploration*, 24: 401-417.

Conventional deconvolution methods are based on the assumption that the seismogram is stationary; however, actual seismic data cannot satisfy the above assumption. Thus, this paper proposes a double deconvolution method in the time-frequency domain to improve the resolution of the non-stationary seismogram. First, the quadratic spectrum modeling method, in combination with the bispectrum method based on higher-order cumulants, was used to extract a wavelet from the non-stationary seismogram, and the spectrum division method was applied to the entire seismogram to perform deconvolution. Then, time-varying wavelets were extracted from the first deconvolution result in the time-frequency domain, and the residual wavelets on every point spectrum were eliminated from the seismogram by a second deconvolution. Simulation experiments and field data processing demonstrated that the proposed method overcomes the interference of adjacent strata effectively and greatly improves the resolution of the non-stationary seismogram.

**KEY WORDS:** double deconvolution method, non-stationary seismogram, time-varying wavelet, quadratic spectral modeling.

## INTRODUCTION

Deconvolution is an important method to describe the detailed stratigraphic structure and enhance the resolution of seismic data processing. Conventional deconvolution methods are often based on the assumption that the seismic signal is stationary and the wavelet is of minimum-phase or zero-phase.

However, scattering and attenuation of the seismic wavelet occurs during the propagation in the underground medium, which results in the lack of high-frequency components and phase distortion of the wavelet, leading to non-stationary seismogram characteristics. Therefore, research on time-varying wavelet extraction methods and time-varying deconvolution methods will be significant for high-resolution seismic data processing (Mirko et al., 2008; Economou et al., 2012).

Rosa et al. (1991) have proposed a variety of spectral modeling deconvolution methods that compress the remaining wavelet and enhance the resolution of the seismic data. The time-frequency domain spectral modeling deconvolution method is one of the most significant methods for overcoming the assumptions of the stationary nature of the seismogram and the phase characteristic of the wavelet. However, due to the sparseness of the reflection coefficient sequence and the interference by neighboring reflection points, fluctuation errors in such time-varying deconvolution methods are caused by the non-sparse condition.

Thus, this study proposes a double deconvolution method in the time-frequency domain that can enhance the resolution of the non-stationary seismogram on the abundant conditions. This method first extracts a mixed-phase wavelet by the quadratic spectral modeling method and bispectrum method based on higher-order cumulants. The spectrum division method is applied to perform deconvolution for the entire non-stationary seismic trace, which could effectively weaken the interference of adjacent strata. The first deconvolution result is then transformed to the time-frequency domain, the residual wavelet is extracted by the mixed phase wavelet extraction method in the time-frequency domain again, and the residual wavelet is eliminated from the seismogram by the second deconvolution, thus enhancing the resolution of the non-stationary seismogram. The workflow of the double deconvolution method is shown in Fig. 1.

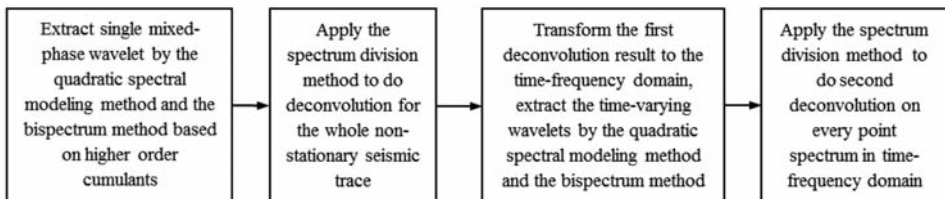


Fig. 1. Workflow of the double deconvolution method in the time-frequency domain.

## WAVELET EXTRACTION AND DECONVOLUTION METHOD

**Wavelet extraction method***1. Extract wavelet amplitude by quadratic spectral modeling*

The common method of wavelet amplitude spectrum estimation is seismogram autocorrelation with the assumption that the reflection coefficient is white noise. Spectral modeling assumes that the amplitude spectrum of the wavelet is smooth and similar to the unimodal curve of the Ricker wavelet spectrum. The empirical mathematical expression of the seismic wavelet is

$$W(f) = |f|^k \exp\left(\sum_{n=0}^N a_n f^n\right) , \quad (1)$$

where  $k$  is a constant,  $a_n$  is the coefficient of the polynomial in  $f$ , and  $N$  is the order number.

This method abandons the assumption of the white-noise reflection coefficient and has shown good results in estimating the wavelet amplitude spectrum and enhancing the resolution of the seismic trace. However, using the fitting polynomial limits the shape of the wavelet amplitude spectrum, which leads to errors at both high and low frequencies in the fitting curve. In addition, the stability of the solution is poor.

Tang et al. (2010) improved the spectral modeling method and proposed a quadratic spectral modeling method to extract the wavelet amplitude. Here, we assume that the convolution model of the seismogram is

$$x(t) = w(t) * r(t) , \quad (2)$$

where  $w(t)$  is the seismic wavelet and  $r(t)$  is the reflection coefficient. The corresponding expression in the frequency domain is

$$A_x(f) = A_w(f)A_r(f) , \quad (3)$$

where  $A_x(f)$ ,  $A_w(f)$  and  $A_r(f)$  denote the amplitude spectrums of the seismogram, wavelet and reflection coefficient, respectively. The following is the Fourier transform of eq. (2)

$$A_x^{(2)}(f) = (1/2\pi)A_w^{(2)}(f) * A_r^{(2)}(f) , \quad (4)$$

where  $A_x^{(2)}(f)$ ,  $A_w^{(2)}(f)$  and  $A_r^{(2)}(f)$  are the amplitude spectra of  $A_x(f)$ ,  $A_w(f)$  and

$A_r(f)$  after the Fourier transform, respectively. The amplitude spectrum is quadratic.

Compared with the traditional spectral modeling methods, this method is highly efficient because the wavelet amplitude extraction is obtained by a one-time Fourier transform. The low-frequency compositions of the seismogram quadratic spectrum then reflect the energy of the seismic wavelet amplitude spectrum, whereas the high-frequency compositions reflect the energy of the reflection coefficient amplitude spectrum. On this basis, we can design a low-pass filter, and the result of filtering the seismogram quadratic spectrum is the wavelet amplitude spectrum. Synthetic examples and actual seismic data processing results show that this method is better than spectral modeling in extracting the time-variant wavelet amplitude spectrum.

Thus, the wavelet amplitude can be extracted by quadratic spectral modeling and combined with the mixed phase, which is obtained by the bispectrum method based on higher-order cumulants and the mixed-phase wavelet is extracted from the entire non-stationary seismogram.

## 2. Extract time-varying wavelet amplitudes in the time-frequency domain

After extracting a time-varying wavelet in the time-frequency domain, the non-stationary seismogram is converted to the time-frequency domain by the improved generalized S transform, and the wavelet amplitudes on every point spectrum can be extracted by quadratic spectral modeling. The mixed phase can be obtained by the bispectrum method based on higher-order cumulants. Thus, the time-varying wavelets could be extracted from a non-stationary seismogram.

The improved generalized S-transform is proposed by Zhang et al. (2011) and its window function is

$$G(t, f) = [1/\sqrt{(2\pi) s |f|^r}] \exp(-t^2/2s^2f^{2r}), \quad s > 0, r > 0, \quad (5)$$

where  $s, r$  are adjustment factors that are greater than zero. Because the width of the Gaussian window is directly proportional to the frequency  $f$ , the window provides high time resolution at low frequencies while providing high frequency resolution at high frequencies, which conforms to the dynamic attenuation characteristics of the seismogram.

Higher time-frequency resolution and focus could be obtained using the improved generalized S-transform to analyze the seismogram, which is conducive to distinguishing changes in the frequency composition of seismic data and intensively analyzing the strata structure. Additionally, the inverse transform can reconstruct the signal without any loss. Therefore, we can process

data effectively in the time-frequency domain and then transform it back into the time domain.

### 3. Extract mixed phase by the bispectrum method

High-order accumulation and high-order spectra include information about the signal that is used to estimate the mixed-phase wavelet (Lazear et al., 1993; Velis et al., 1996). Based on the nature of the high-order statistics, the mixed-phase wavelet spectrum can be extracted by the seismogram bispectrum.

There are many algorithms for computing the wavelet phase from the bispectrum of the seismogram, such as the Brilliger algorithm, Lii-Rosenblatt algorithm and Matsuura-Ulrych algorithm. The Brilliger algorithm is recursive and sensitive to errors in the estimated initial value. The Lii-Rosenblatt algorithm relies only on part of the bispectrum values. The Matsuura-Ulrych algorithm utilizes all bispectral values and does not have cumulative errors. Therefore, in this paper, we choose the latter algorithm.

Assuming that is a non-stationary random process of zero mean, its three-order cumulants are

$$c_{3x}(\alpha_1, \alpha_2) = E[x(k)x(k + \alpha_1), x(k + \alpha_2)] \quad (6)$$

After Fourier transforming, we obtain the three-order spectrum of  $x(k)$ , namely, the bispectrum. Its amplitude and phase spectra are

$$|B_x(\omega_1, \omega_2)| = |X(\omega_1)| |X(\omega_2)| |X(\omega_1 + \omega_2)| \quad (7)$$

$$\psi(\omega_1, \omega_2) = \phi(\omega_1) + \phi(\omega_2) - \phi(\omega_1 + \omega_2) \quad (8)$$

where  $\phi(\omega)$  is the phase spectrum and  $|X(\omega)|$  is the amplitude spectrum.

Based on the convolution model, the seismic reflection record is as follows:

$$x(t) = r(t) * w(t) \quad (9)$$

where  $r(t)$  is the reflection coefficient and  $w(t)$  is the seismic wavelet. Based on the nature of the bispectrum, we can obtain

$$B_x(\omega_1, \omega_2) = B_r(\omega_1, \omega_2) B_w(\omega_1, \omega_2) \quad (10)$$

where  $B_r(\omega_1, \omega_2) = \sigma^2$ , a mean square, when the reflection coefficient is a white process. There is only a proportional coefficient between the wavelet bispectrum

and seismogram bispectrum, which allows us to obtain the wavelet bispectrum from the seismogram bispectrum. If the wavelet spectrum is expressed by

$$W(\omega) = |W(\omega)| \exp[i\varphi(\omega)] \quad , \quad (11)$$

where  $\varphi(\omega)$  and  $|W(\omega)|$  are the phase spectrum and amplitude spectrum of  $w(t)$ , respectively. According to eq. (8),

$$\psi(\omega_1, \omega_2) = \varphi(\omega_1) + \varphi(\omega_2) - \varphi(\omega_1 + \omega_2) \quad . \quad (12)$$

The mixed phase can be extracted from the non-stationary seismogram by the bispectrum method using the Matsuura-Ulrych algorithm (Pan et al., 1987). Mixed-phase wavelets could be fitted with the extracted amplitudes.

### Deconvolution method

As deconvolution is an important tool for testing the accuracy of the extracted wavelet, the research on deconvolution methods suitable for non-stationary seismograms is an important part of enhancing the resolution.

Existing deterministic deconvolution methods are rather mature, such as the least squares deconvolution, minimum entropy deconvolution (Wiggins, 1978), sparse spike deconvolution (Sacchi, 1997), multi-resolution seismic signal deconvolution, and trace inversion (Zhang, 2011). The time-domain deconvolution is inevitable to truncate the wavelet because the wavelet is an infinite impulse response sequence described by an autoregressive moving average (ARMA) model. To reduce the truncation error on the inversion process, we choose the spectrum division method in the frequency domain for deconvolution after extracting the time-varying wavelets.

The Robinson convolution model can be obtained through Fourier transform as follows:

$$X(e^{j\omega}) = W(e^{j\omega})R(e^{j\omega}) \quad , \quad (13)$$

where  $X(e^{j\omega})$ ,  $W(e^{j\omega})$  and  $R(e^{j\omega})$  denote the seismogram, wavelet and reflection coefficient sequence expressed in the frequency domain, respectively. The reflection coefficient sequence can be expressed as

$$\tilde{r}(n) = F^{-1}[\tilde{R}(e^{j\omega})] = F^{-1}[X(e^{j\omega})/\tilde{W}(e^{j\omega})] \quad (14)$$

where  $\tilde{r}(n)$  and  $\tilde{R}(e^{j\omega})$  are the reflection coefficient estimations in the time domain and frequency domain, respectively.  $F^{-1}$  is the inverse Fourier transform operator and  $\tilde{W}(e^{j\omega})$  is the estimated wavelet expressed in the frequency domain.

After extracting one mixed-phase wavelet from the non-stationary seismogram using the quadratic spectral modeling method and bispectrum method based on higher-order cumulants, the spectrum division method is used to perform the first deconvolution of the entire non-stationary seismic trace; this deconvolution could effectively weaken the interference of adjacent strata. Then, the first deconvolution result is transformed into the time-frequency domain by the improved generalized S transform, and time-varying wavelets are extracted in the time-frequency domain again. The residual wavelet is then eliminated from the seismogram by the second deconvolution, thus enhancing the resolution of the non-stationary seismogram.

## ANALYSIS OF THE SIMULATION RESULTS

### Limitations of the traditional time-varying deconvolution method

The traditional time-varying deconvolution methods based on spectrum modeling could overcome the assumptions that the seismogram is stationary and the wavelet is of zero or minimum phase, which have significant effects on enhancing the seismogram resolution by compressing the wavelet. However, such methods also have limitations, which require a higher sparse feature of the reflection coefficient sequence.

To illustrate the existing limitations of the traditional time-frequency domain deconvolution methods, two non-stationary seismograms are constructed based on the sparse and non-sparse reflection coefficient sequences combined with the zero-phase wavelet (Kumar et al., 2008). Time-varying wavelets are extracted from the non-stationary seismograms based on the quadratic spectral modeling method in the time-frequency domain. Then, the spectrum division method is used to process deconvolution for the seismograms on every point spectrum; the results are shown in Fig. 2.

Fig. 2 illustrates that in the case of the sparse reflection coefficient, the wavelet component is greatly weakened by the spectrum division on every point spectrum and the obtained seismogram is closer to the pulse sequence at the reflection point. In contrast, in the case of the non-sparse reflection coefficient, the seismogram from the spectrum division has large fluctuation errors (indicated by arrows). The time-varying deconvolution method of spectrum division is better in the case of the sparse reflection coefficient, but there is a large error when the reflection coefficient does not satisfy the sparse condition.

## Double deconvolution method in the time-frequency domain

To solve the problems of the traditional time-varying deconvolution methods, a double deconvolution method in the time-frequency domain is proposed to enhance the resolution of the non-stationary seismogram. An autoregressive moving average (ARMA) model is used to describe the seismic wavelet. The synthetic non-stationary seismogram is structured based on a convolution model by the mixed phase wavelet. Fig. 3 shows the mixed phase wavelet (a), reflection coefficient sequence (b) and non-stationary seismogram (c).

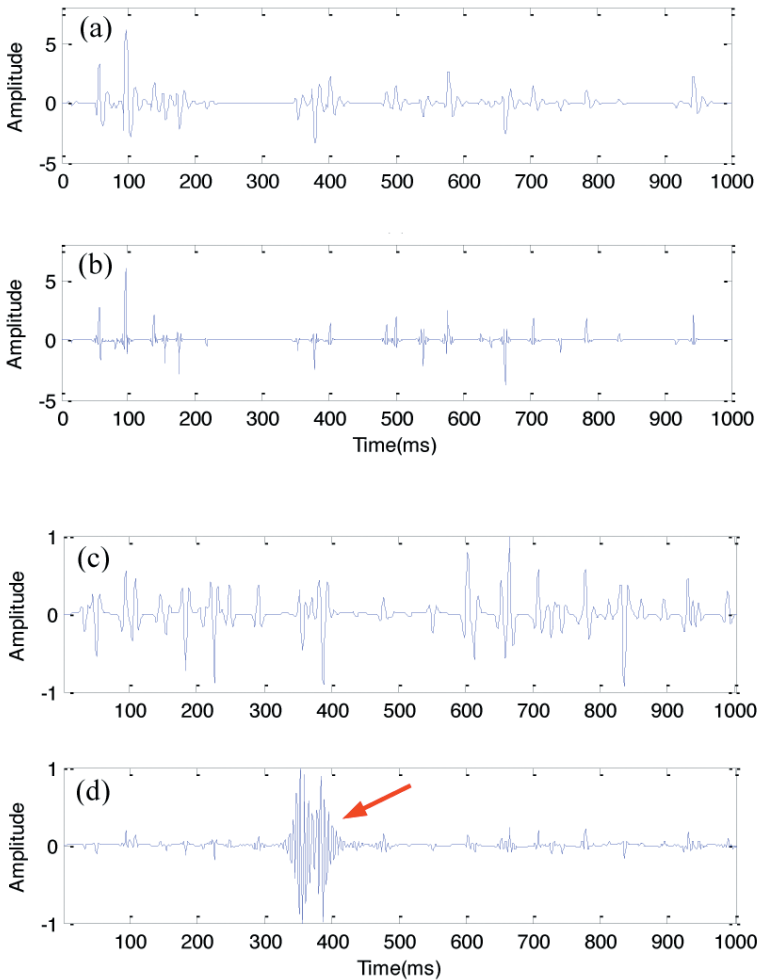


Fig. 2. Non-stationary seismogram based on the sparse reflection coefficient sequence (a) and its deconvolution result (b). Non-stationary seismogram based on the non-sparse reflection coefficient sequence (c) and its deconvolution result (d).



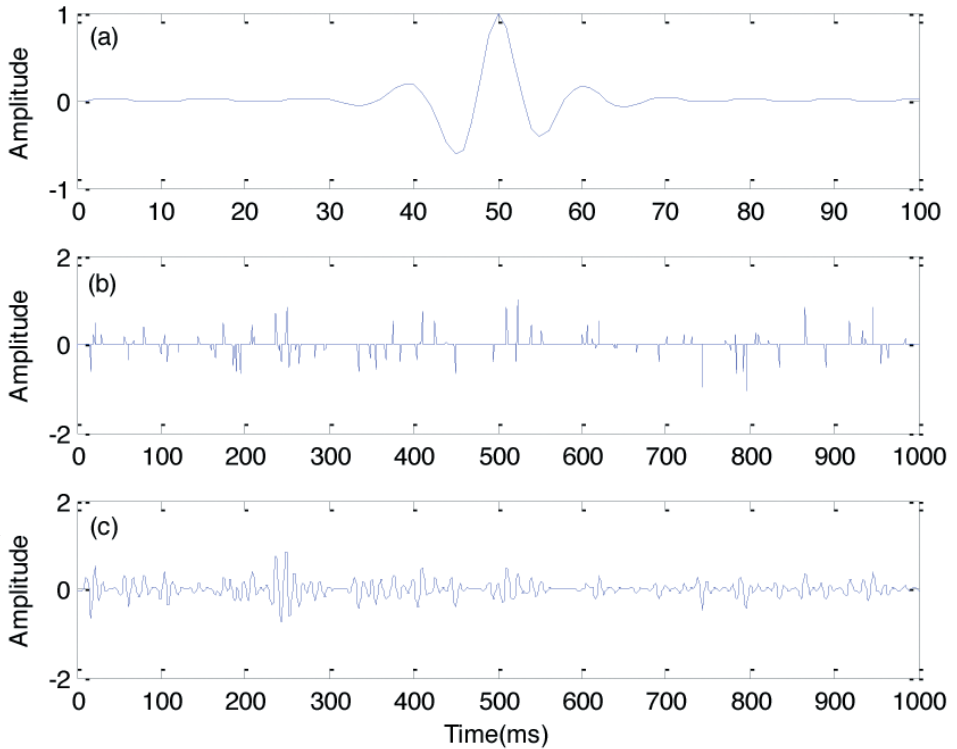


Fig. 3. (a) Original wavelet, (b) reflection coefficient sequence, and (c) synthetic non-stationary seismogram.

### 1. Analysis of the first deconvolution result

The wavelet amplitude from the non-stationary seismogram, shown in Fig. 3(c), can be extracted by quadratic spectral modeling, and the mixed phase can be estimated by the bispectrum method based on higher-order cumulants. The extracted wavelet is shown in Fig. 4. The spectrum division method is applied to process deconvolution for the entire seismogram, which is shown in Fig. 5. The actual reflection coefficient, the deconvolution result and the difference between the deconvolution result and the actual reflection coefficient are shown in Fig. 5.

Figs. 4 and 5 show that the basic form of the extracted wavelet is consistent with that of the original wavelet. However, there are some differences between the estimated wavelet and the original wavelet, indicated by arrows. These differences illustrate the distortion that occurs during the propagation of the wavelet, which is mainly caused by the non-stationary nature of the seismogram. Furthermore, valid signals are not identified in the difference

result, which illustrates that the valid signal is retained well by the first deconvolution. The pulse feature is significantly enhanced by the first deconvolution compared to the original non-stationary seismogram, and the wavelet influence is effectively suppressed. Finally, the first deconvolution result has weaker noise, but its resolution is not sufficiently high to distinguish all the layers, indicating that subsequent processing is required.

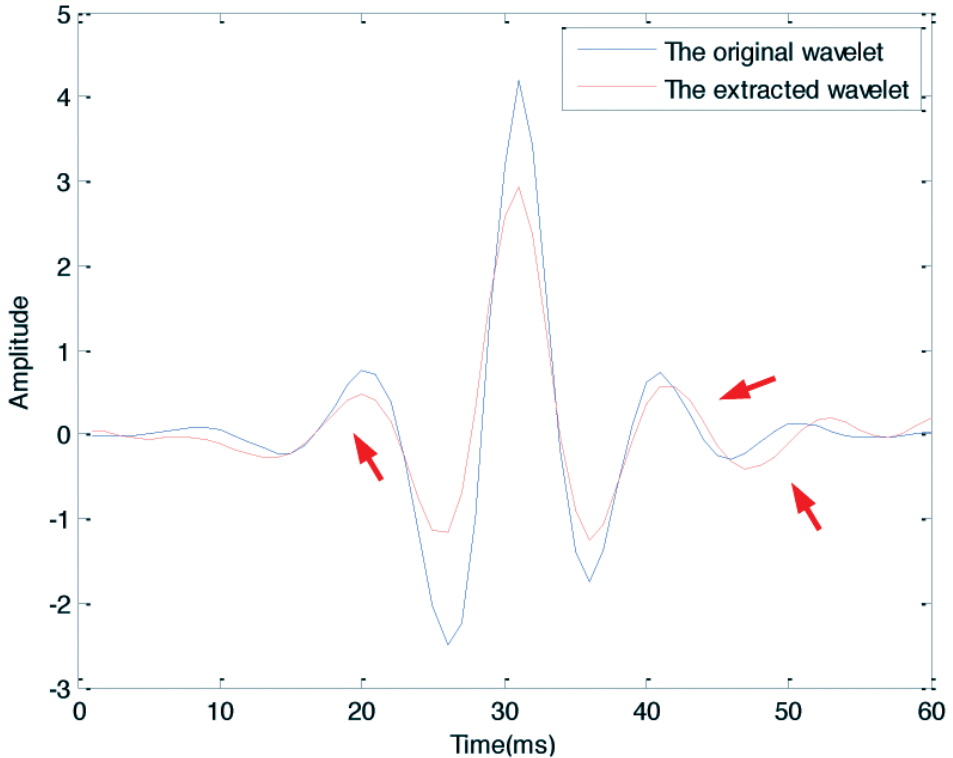


Fig. 4. Extracted wavelet based on spectrum modeling.

## 2. Analysis of the second deconvolution result

For the first deconvolution result shown in Fig. 5, the wavelet amplitude of every point can be extracted by quadratic spectral modeling, and the mixed phase can be estimated by the bispectrum method based on higher-order cumulants on every point spectrum. The spectrum division method in the frequency domain is used to process the second deconvolution after extracting time-varying wavelets in the time-frequency domain.

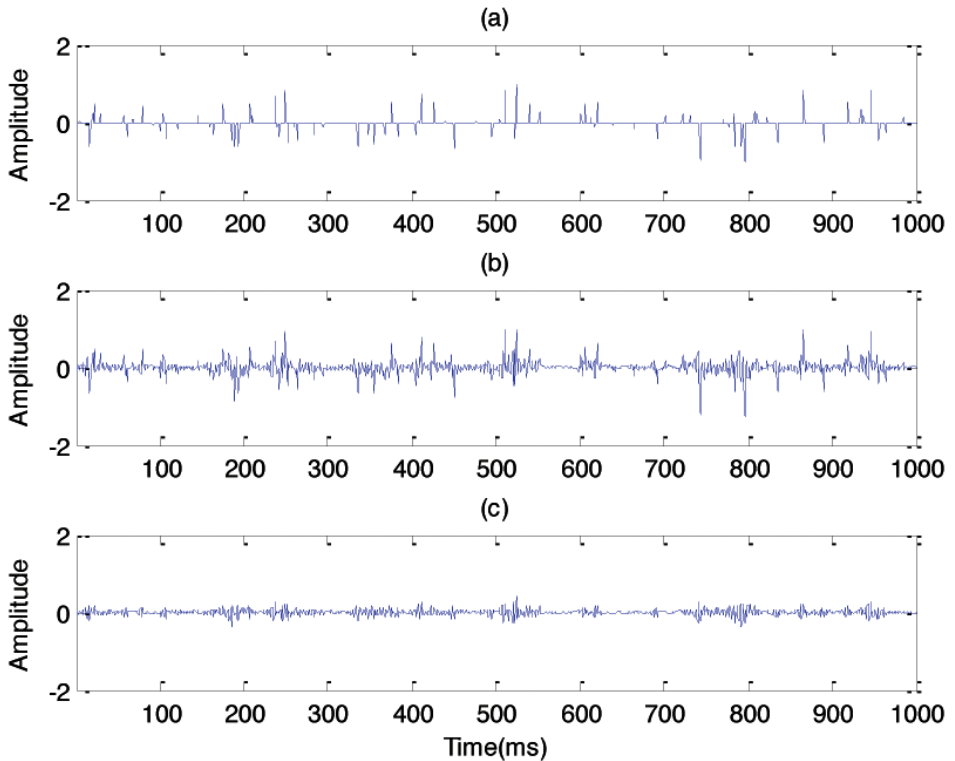


Fig. 5. (a) Actual reflection coefficient, (b) deconvolution result, (c) difference between the deconvolution result and actual reflection coefficient.

After transforming the first deconvolution result shown in Fig. 5 into the time-frequency domain using the improved generalized S-transform, the wavelet amplitude spectrum on every point spectrum is extracted from the seismogram by quadratic spectral modeling in the time-frequency domain. Fig. 6 shows the amplitude spectra of the original wavelet, the first deconvolution result and the extracted wavelets by quadratic spectral modeling at 100 ms (a), 500 ms (b), 520 ms (c) and 900 ms (d).

Fig. 6 illustrates that early on ( $t = 100$  ms), amplitude spectra are consistent with that of the original wavelet. However, over time, the main frequency and amplitude of the extracted wavelet decrease, which reflects the dynamic attenuation nature of the wavelet when propagating.

The wavelet amplitude of every point can be extracted by quadratic spectral modeling, and the mixed phase can be estimated by the bispectrum method based on higher-order cumulants. The extracted time-varying wavelets (100, 500, 520, and 900 ms) of the first deconvolution result and the original wavelet are shown in Fig. 7.

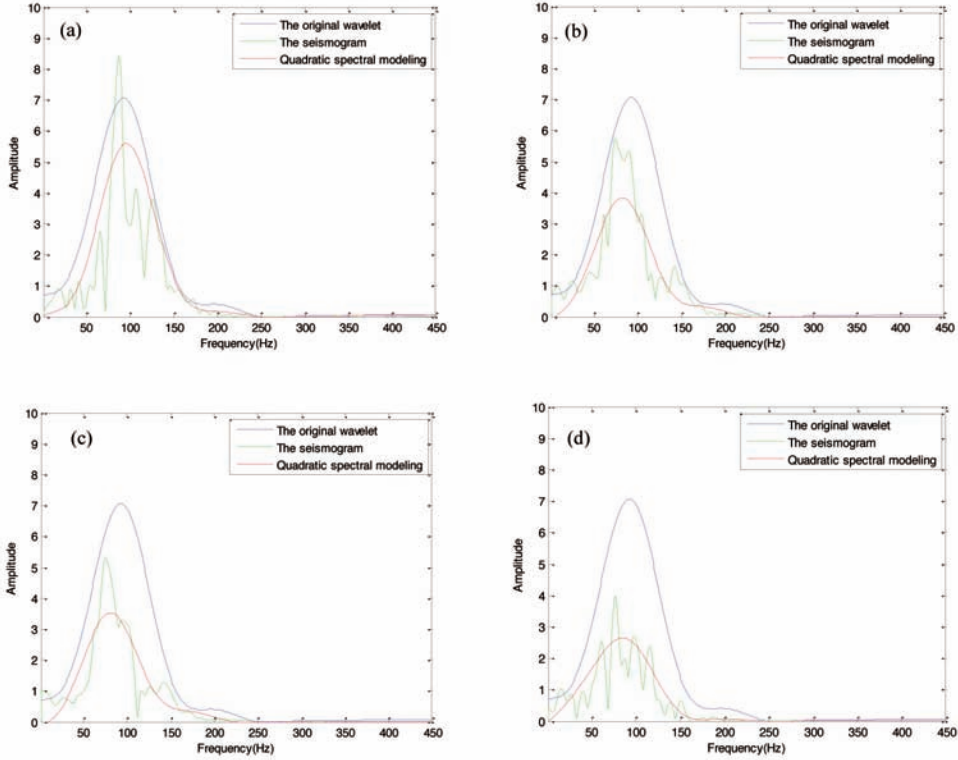


Fig. 6. Time-frequency domain spectral contrast at (a) 100 ms, (b) 500 ms, (c) 520 ms and (d) 900 ms.

Fig. 7 shows that early on ( $t = 100$  ms), the time-domain waveform of wavelets extracted from the time-frequency domain is consistent with the original wavelet. Over time, the main frequency and amplitude of the extracted wavelet decrease, which reflects the dynamic attenuation nature of the wavelet when propagating. At 500 and 520 ms, it is difficult to identify the wavelets because the layers are in close proximity. However, there are better wavelet extraction results in these two points, which illustrates that the method can accurately extract the wavelet at each reflection point.

The spectrum division method in the frequency domain is applied to process second deconvolution after extracting time-varying wavelets at every point in the time-frequency domain. The double deconvolution result is shown in Fig. 8. The conventional spectrum modeling deconvolution method is tested to verify the superiority of the proposed method. The conventional deconvolution result is shown in Fig. 9.

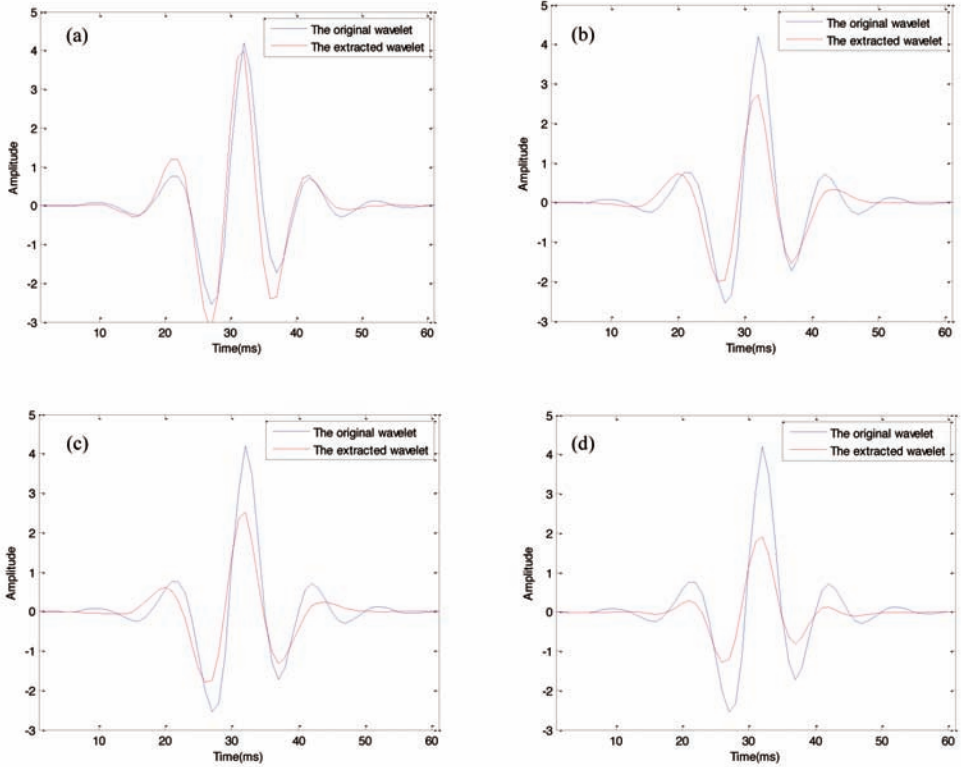


Fig. 7. Time-domain waveforms of wavelets at (a) 100 ms, (b) 500 ms, (c) 520 ms and (d) 900 ms.

Figs. 8 and 9 show that the second deconvolution result in the time-frequency domain has nearly no noise. The horizon is clear, and it is closer to the actual reflection coefficient. The double deconvolution method in the time-frequency domain eliminates the interference errors from direct deconvolution by spectrum division, and the deconvolution result is closer to the pulse sequence. Furthermore, we can distinguish most of the horizons from deconvolution results from conventional spectrum modeling deconvolution. Due to noise interference, some thin horizons and horizons with small reflection coefficients (indicated by arrows) are difficult to distinguish. Finally, valid signals are not identified in the difference result, which illustrates that we can obtain a more accurate reflection coefficient based on the proposed double deconvolution method in the time-frequency domain.

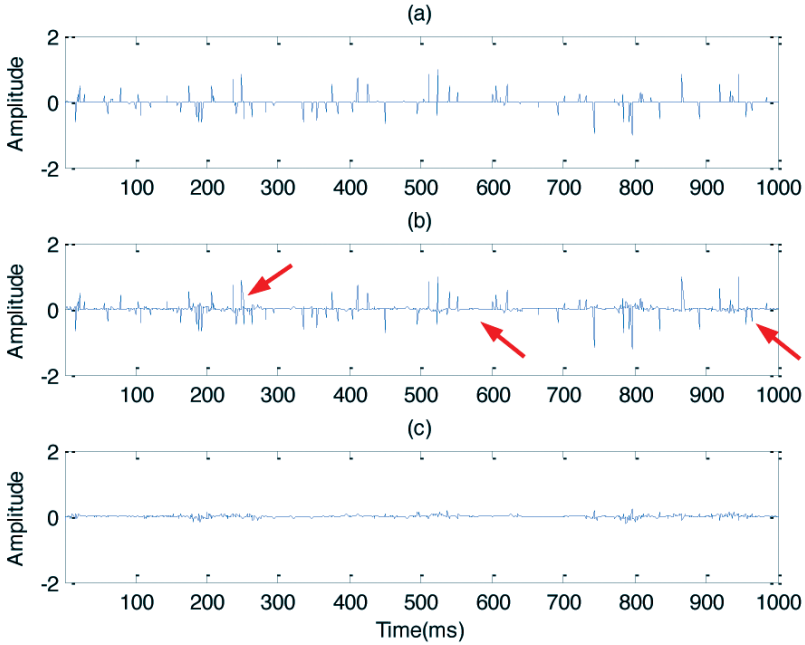


Fig. 8. (a) Actual reflection coefficient, (b) double deconvolution result, (c) difference between the double deconvolution result and actual reflection coefficient.

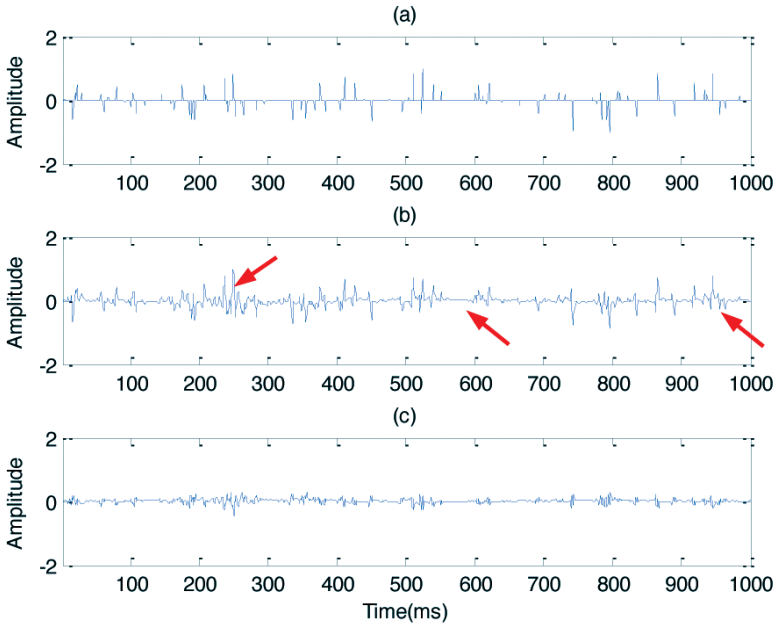


Fig. 9. (a) Actual reflection coefficient, (b) conventional spectrum modeling deconvolution result, (c) difference between the deconvolution result and actual reflection coefficient.

## ANALYSIS OF ACTUAL SEISMIC DATA PROCESSING

Fig. 10(a) is a seismic section of the Shengli Oil Field with 261 traces and a sampling interval of 2 ms. The 189th trace is extracted and shown in Fig. 10(b), and the reflection coefficient sequences from logging are shown in Fig. 10(c). First, a mixed-phase wavelet is extracted by the quadratic spectrum modeling method combined with the bispectrum method from the non-stationary seismogram, and the spectrum division method is applied to the entire seismogram to obtain a deconvolution result. Then, the residual wavelet is evaluated by the mixed phase wavelet extraction method in the time-frequency domain, and the residual wavelet is eliminated from the seismogram by the second deconvolution, thus enhancing the resolution of the non-stationary seismogram. Fig. 11 shows the extracted wavelets, and Fig. 12 shows the double deconvolution results.

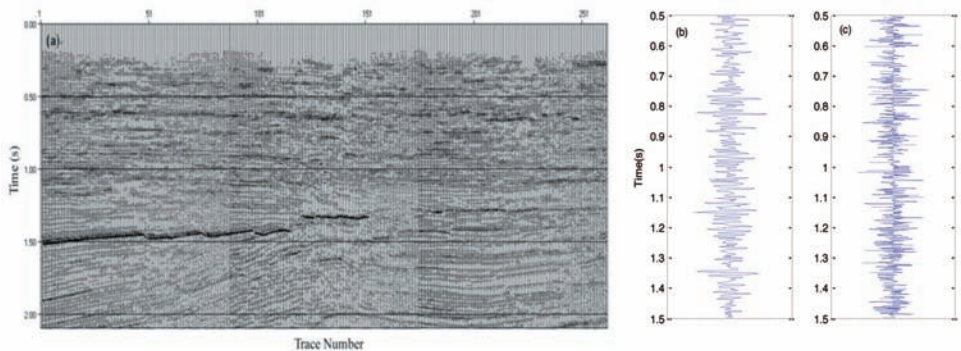


Fig. 10. (a) Actual seismic section of Shengli Oil Field; (b) 189th seismic trace; (c) reflection coefficient sequences from logging.

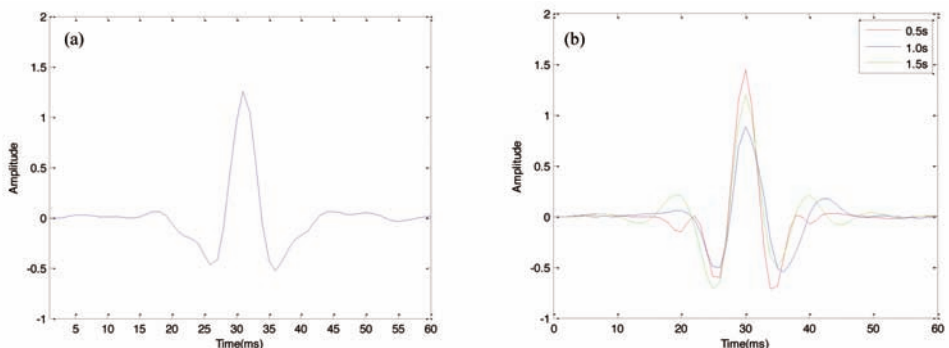


Fig. 11. (a) Extracted wavelet of the entire seismic trace; (b) extracted time-varying wavelets.

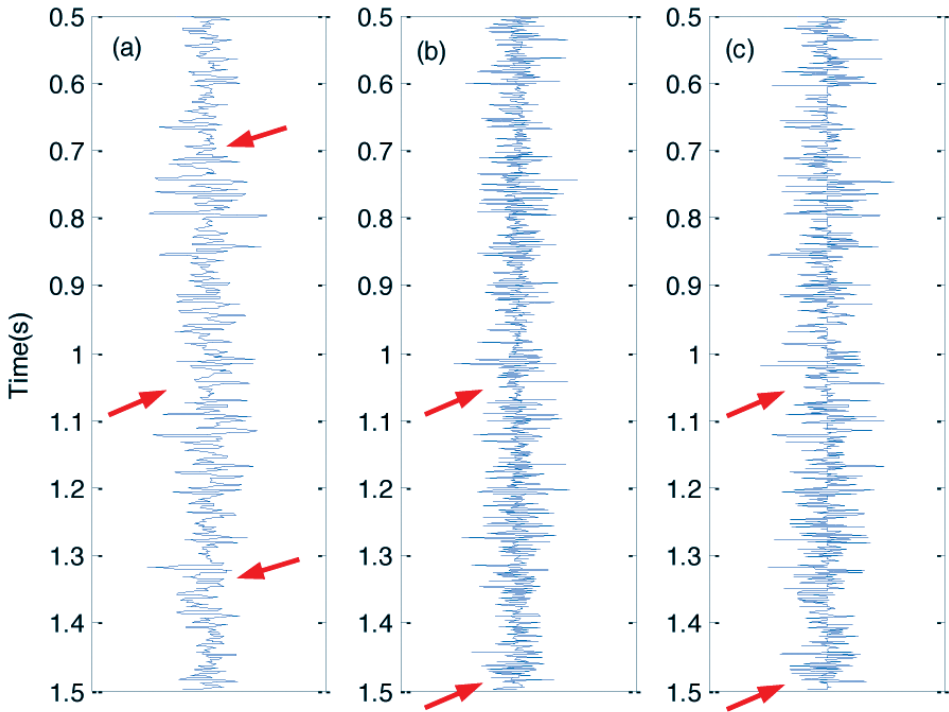


Fig. 12. (a) Conventional deconvolution result; (b) double deconvolution result; (c) reflection coefficient sequences from logging.

Fig. 12 illustrates that the pulse feature of the conventional deconvolution result is significantly enhanced compared to the original seismogram. However, there is inevitably noise in the inversion result, which leads to the trace bend [indicated by arrows in Fig. 12(a)] produced in some parts. Furthermore, the double deconvolution result has a higher signal-to-noise ratio, the stratigraphy is easier to discriminate, and the pulse feature of the reflection coefficient sequence is more notable. Thus, the proposed method is suitable for actual seismic data processing. Finally, as indicated by the arrows shown in Figs. 12(b) and 12(c), the double deconvolution result still has some interference, and more effective methods must be investigated.

## CONCLUSION

In this study, a double deconvolution method in the time-frequency domain is proposed to overcome the limitations of traditional time-varying deconvolution methods. Several conclusions can be drawn from the simulations



and actual seismic data processing. The double deconvolution results demonstrate that the first deconvolution suitably weakens the interference of adjacent strata and that the second deconvolution could remove the effect of the wavelet, greatly enhancing the seismogram resolution. Thus, the proposed method of double deconvolution in the time-frequency domain is robust, practical, and applicable to actual seismic data.

Because seismic data are typically subjected to interference noise that affects the deconvolution result, a deconvolution method with strong anti-noise ability must be studied further.

## ACKNOWLEDGEMENTS

This work was supported by the National Natural Science Foundation of China (40974072) and China University of Petroleum (east China) graduate student innovation project funding (YCX2015050). The authors gratefully acknowledge their financial support.

## REFERENCES

- Economou, N. and Vafidis, A., 2012. GPR data time varying deconvolution by Kurtosis maximization. *J. Appl. Geophys.*, 81: 117-121.
- Kumar, V. and Herrmann, F.J., 2008. Deconvolution with curvelet-domain sparsity, Expanded Abstr., 78th Ann. Internat. SEG Mtg., Las Vegas, 27(1): 1996-2000.
- Lazear, G.D., 1993. Mixed-phase wavelet estimation using fourth-order cumulants. *Geophysics*, 58: 1042-1051.
- van der Baan, M., 2008. Time-varying wavelet estimation and deconvolution by Kurtosis maximization. *Geophysics*, 73(2): 11-18.
- Pan, R. and Nikiyas, C.L., 1987. Phase reconstruction in the trispectrum domain. *Acoust., Speech Signal Process., IEEE Transact.*, 35: 895-897.
- Rosa, A.L.R. and Ulrych, T.J., 1991. Processing via spectral modeling. *Geophysics*, 56: 1224-1251.
- Sacchi, M.D., 1997. Re-weighting strategies in seismic deconvolution. *Geophys. J. Internat.*, 12(9): 651-656.
- Tang, B.W, Zhao, B., Wu, Y.H. and Li, H.Q., 2010. A new way to realize spectral modeling deconvolution. *Oil Geophys. Prospect.* (in Chinese), 45: 66-70.
- Velis, D.R. and Ulrych, T.J., 1996. Simulated annealing wavelet estimation via fourth-order cumulant matching. *Geophysics*, 61: 1939-1948.
- Wiggins, R., 1978. Minimum entropy deconvolution. *Geoexplor.*, 16(5): 21-35.
- Zhang, G., Li, Y., Rong, J., Zhang, Y. and Cai, Z., 2011. Compensation for stratigraphic absorption of seismic attenuation based on the improved generalized S-transform. 73rd EAGE Conf., Vienna.
- Zhang, R. and Castagna, J., 2011. Seismic sparse-layer reflectivity inversion using basis pursuit decomposition. *Geophysics*, 76(6): 147-158.